Investigating the Effects of Noise on a Cell-to-Cell Communication Mechanism for Structure Regeneration

Giordano B. S. Ferreira[1], Matthias Scheutz[1] and Michael Levin[2]

[1]Human Robot Interaction Laboratory at Tufts University, Medford, MA 02155
[2]Allen Discovery Center at Tufts University, Medford, MA 02155
{giordano.ferreira, matthias.scheutz, michael.levin}@tufts.edu

Abstract

In this paper we modified a previous cell-cell communication mechanism of dynamic structure discovery and regeneration to account for the presence of noise that could alter the route of messages transmitted across cells. We report results from a large number of simulation runs where noise was applied to the distance and direction of messages dispatched by cells. Based on our analysis of the results, we proposed an "activation" mechanism where missing cells need to receive a certain number of messages first before they divide and recreate missing cells. We then show that, due to the inherent message redundancy in the organism this mechanism improved the performance of the model even when noise is present on packets.

Introduction

Several biological organisms are capable of regenerating some of their cellular structures. For example, it is well-known that some animals can fully regrow their liver after the removal of two thirds of its tissue (Higgins, 1931), deer can regrow the correct pattern of their antlers at a rate of over 1 cm/day of new bone, nerve and skin (Price et al., 2005), and planarian flatworms can recover their shapes from any fragment of the body as small as $\frac{1}{279^{th}}$ of their entire area (Morgan, 1898). Regeneration of complex pattern (as distinct from simple wound healing) requires group decision-making that coordinates cells toward forming the right anatomical structures of the correct size, contents, and topological relationship to the rest of the tissue (Birnbaum and Alvarado, 2008). Understanding the dynamics that guide regenerative processes will shed light on other research areas such as regenerative medicine, aging, birth defects, and even the pattern dysregulation known as cancer.

Progress has been made in explaining some aspects of the regeneration process using models of gene regulation (Umesono et al., 2013; Werner et al., 2015; Owlarn and Bartscherer, 2016). Although it is important to identify gene products involved in (necessary for) regeneration, future progress in evolutionary biology, biomedicine, and synthetic bioengineering requires gaining algorithmic understanding of how a network of cells maintains information about the large-scale shape of the organism and correctly creates missing structures (Levin, 2012).

Cell-cell communication is a crucial aspect of this process. For example, planarian flatworms bisected at any point along their length will give rise to normal worms: the anterior-facing wound makes a head, while the posterior-facing wound makes a tail. The cut ends of each fragment create radically different anatomical structures despite the fact that they were adjacent neighbors before the cut. Thus, the information needed to make this anatomical decision is not local (cannot be specified by positional information, which is the same for wounds on either side of the scalpel cut). Instead, the wound cells must communicate with the rest of the body to determine which structures to make based on what is present and where the wound is located with respect to the remaining body. This information must be computed in real time during the life of the animal (the genome encodes the computational machinery to cope with unpredictable injuries).

Importantly, the target morphology (TM, the shape to which an animal regenerates upon damage) of a given animal is not invariant - it is not hardcoded, nor is it directly specified in the genome (Levin, 2014). It is well-known that genomes do not specify shape directly; anatomy is an emergent feature of the computational and physical processes carried out by the proteins encoded with the genome. Less well-appreciated is the fact that this middle layer between the genome and the anatomical outcomes is an attractive and tractable target for interventions that can alter anatomy from its genome-default outcome despite a normal wild-time genetic sequence (Levin, 2013; Sullivan et al., 2016). Research on long-term changes of regenerative pattern has revealed that the target morphology can be altered and re-written, without editing the genomic sequence (reviewed in Lobo et al. (2014)). For instance, studies with deer showed that localized injury (not mutation) of a deer's antlers result in ectopic branches at that same location, in subsequent years of antler regrowth, revealing a pattern memory that can be altered by experience not requiring genetic change (Bubenik, 1990). Similarly, planarian flatworms can be converted to a

Carole Knibbe et al, eds., Proceedings of the ECAL 2017, Lyon, France, 4-8 September 2017,
(Cambridge, MA: The MIT Press, ©2017 Massachusetts Institute of Technology).

permanent biaxial two-headed form after a brief (transient) physiological perturbation of the cells' electrical connectivity (Oviedo et al., 2010). More recent work reveals how endogenous bioelectric states within tissues serve as instructive elements that specify regenerative patterns for future rounds of injury (Durant et al., 2017). A significant body of knowledge now reveals how real-time signaling among cell groups can alter the patterning of embryogenesis, regeneration, and remodeling from its default TM despite a wild-type genome (Herrera-Rincon et al., 2017; Sullivan et al., 2016).

These kinds of stable changes to the TM without genomic editing, occurring during the life span of an organism, reveal the importance of dynamic cell-cell communication networks for establishing large-scale anatomy (Sullivan et al., 2016). Likewise, the disorganization of patterning has been suggested as a source of the systems-level circuit disorder that leads to cancer (Chernet and Levin, 2013; Soto and Sonnenschein, 2005; Huang et al., 2009). Rational control of growth and form, for biomedical purposes as well as synthetic bioengineering, thus requires addressing a major gap in this field: the dearth of models of communication during regenerative decision-making, especially those that are algorithmic (are sufficiently specified to be used as simulations that can generate predictions).

In Ferreira et al. (2016), we introduced a cell-cell communication mechanism by which cells perfectly communicate with their neighbors and could therefore dynamically discover and maintain the structure of a group of cells while some cells randomly die. In another set of experiments, we confirmed that even for cuts that removed tissue areas as large as half of the organism this communication mechanism could regenerate the entire shape. The communication mechanism consists of cells exchanging morphological information – defined here as "packets" – among neighbors and then using this information to regenerate any missing part in the shape of the organism. We implemented this mechanism in an agent-based model (ABM) in which cells are modeled as agents that send packets to and receive packets from their neighbors. Packets travel across the structure in order to trace and discover the morphological shape. The set of existing packets at any given time can be seen to describe some aspect of the shape of the organism because all packets previously passed through at least one cell. Thus, after a packet has traveled through the structure for a while, it returns (i.e., backtracks) on the same path along which it had previously traveled. If there is a missing cell in any position along the path, the cell that needs to relay this packet to the missing cell starts to divide and regrows a new cell in that position of the missing cell, thus completing the path.

Figure 1 shows a functional diagram of the cell-cell communication model.[1] The simulation iterates through all cells sensing all packets received from neighbors, as well as all packets held in the last cycle and the new packets this cell creates in this cycle (defined by the parameter $PacketFreq$). This process persists until the current cycle is different from the defined maximum number of cycles. For each packet the cell sensed, the cell decides the next owner of this packet in the next cycle. Each parameter then plays a role in this decision. First, $MinBends$ determines when the packet has to backtrack (i.e., after this cycle, the packet will start to regenerate missing cells). $MinTopLengthToHold$ and $HoldProb$ determine whether the packet will be held in the next cycle (i.e., will remain in the same cell). $BendProb$ defines the probability of a packet changing direction (i.e., bending). In summary, $PacketFreq$ defines the number of new packets each cell creates at each cycle. $MinBends$ and $BendProb$ define the variability of the packet's path in the structure. Finally, $MinTopLengthToHold$ and $HoldProb$ define how long a packet can stay in the structure.

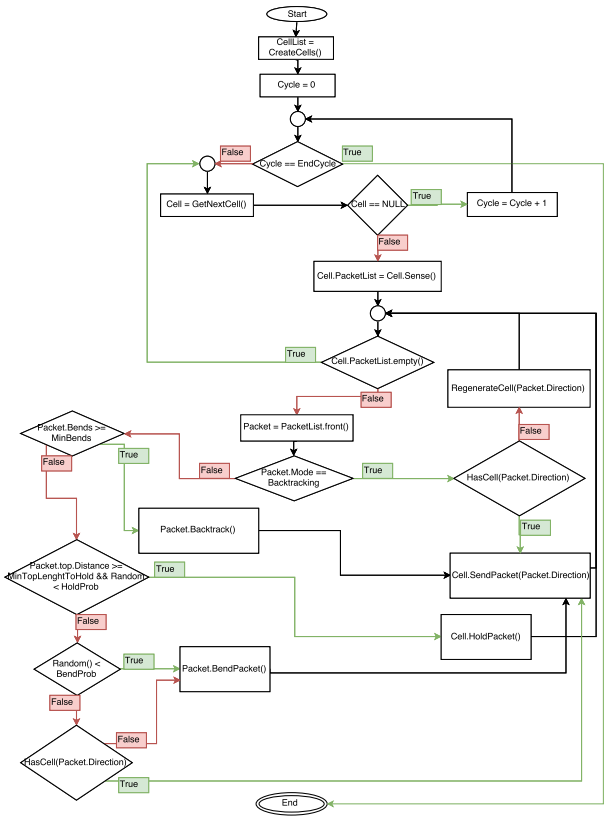

Figure 1: Functional diagram of the cell-cell communication model.

In Ferreira et al. (2016) we did not want to map the mechanism to a specific biological process, but instead proposed a new procedure by which cells could obtain, store, and then use morphological information to repair the arrangement of those cells. However, a first step towards finding a mapping

[1]The version of the simulator used in this paper can be downloaded from: http://hrilab.tufts.edu/software/ecal17.zip

Carole Knibbe et al, eds., Proceedings of the ECAL 2017, Lyon, France, 4-8 September 2017,
(Cambridge, MA: The MIT Press, ©2017 Massachusetts Institute of Technology).

from the model mechanism to cell communication mechanisms (if such a mapping exists) is to verify the reliability of the model mechanism under conditions of noise that could affect the routing process performed by packets exchanged between cells. Thus, in this paper we are interested in exploring the effects of noise regarding the distance and direction those packets travel across the structure. To do that, we implemented the previous cell-cell communication mechanism in a 3D group of cells with a shape resembling the planarian worm. We then performed a cut to remove the top part of the simulated worm and verified if the mechanism was capable of regrowing all missing cells even though some packets were not perfectly transmitted.

Experiments with Noise on Packets

We added independent Gaussian noise in the packet distance and direction according to the parameters $\sigma_{DistanceNoise}$ and $\sigma_{DirectionNoise}$. At the moment the packet starts backtracking, both noise elements are independently applied to each vector in the packet. The distance noise $n^v_{Distance}$ is calculated by a Gaussian distribution with mean $\mu_{Distance} = 0$ and standard deviation $\sigma_{DistanceNoise}$. Then $floor(n^v_{distance})$ is added to the distance of vector $v_{Distance}$. Therefore, after applying noise, the packet can either backtrack by the same number of cells, by a longer distance or a shorter distance. The direction noise $n^v_{Direction}$ is also calculated based on a Gaussian distribution with mean $\mu_{Direction} = 0$ and standard deviation $\sigma_{DirectionNoise}$. If $abs(n^v_{Direction}) \geq 1$ then the packet changes direction, otherwise it maintains its original direction. Thus, if the noise modifies the direction of vector v, this new direction is uniformly selected from the four options in which the sender and receiver cells have the same neighbors.

We expected to see some "overgrowth" in the shape of the organism due to noise applied on packets for the following reasons: first, if a packet that passes through one cell on the edges of the worm backtracks by a longer distance than it is supposed to, new cells will be created in that direction; second, if due to noise a packet near one edge changes its direction (e.g., a packet in the topmost layer has a vector v with $v_{Direction} = east$ and $v_{Distance} = 10$ and noise changes the direction of v to a supposed neighbor on top of the cell, this packet will create 10 cells on the top of the worm). Thus, there are two goals for these evaluation experiments: first, we need to confirm the reliability of the model even when noise is applied to packets and second, we need to compare the similarity between the original worm and the regenerated worm when noise causes overgrowth. Thus, there are two dependent variables of our model: *RegenerationRatio* and *Sim*. The *RegenerationRatio* is the proportion of regenerated cells over removed cells (equation 1).

$$RegenerationRatio = \frac{RegeneratedCells}{RemovedCells} \quad (1)$$

where *RemovedCells* is the number of cells removed by the cut, including any overgrowth. *RegeneratedCells* is the number of cells regenerated in positions that had removed cells. Therefore, a value of $RegenerationRatio = 1$ represents full regeneration of the worm that existed at the moment of the cut.

However, it is also important to verify how similar the regenerated worm is to its original shape. For instance, we need to verify whether the worm has missing cells in positions where cells previously existed, or whether the worm has cells in locations where no cells existed before. Equation 2 shows the similarity metric Sim.

$$Sim = \frac{AliveCells - (Overgrowth + MissingCells)}{TotalCells} \quad (2)$$

where *TotalCells* is the total number of cells in the organism. *AliveCells* is the number of alive cells in locations where there was a cell in the original worm. *Overgrowth* is the number of alive cells in locations where there was not an alive cell in the original shape (i.e., cells that grew due to noise). *MissingCells* is the number of locations where there existed a cell in the original worm, but the model did not get to regrow a new cell. Therefore, a value of $Sim = 1$ represents a full regeneration with no overgrowth.

To explore the performance of the model with the two metrics, we fixed some model parameters and varied others. Specifically, we fixed the parameters related to cells holding packets, since they are not affected by the applied noise, $MinTopLen = 3$ and $HoldProb = 0.5$. Hence, packets with top vector longer than 3 cells could be held with 50% probability. We also fixed a 3D planarian-like structure with three distinct areas grouped together: a head containing 167 cells per layer, a body containing 255 cells per layer and a tail containing 103 cells per layer. It is worth noting that although cells belong to different groups, they have no structural or functional differences. The structure contains 4 layers stacked on top of each other, totaling 2100 cells. Figure 2 shows the topmost layer with the three groups of cells highlighted. We performed a cut on the worm structure in which we removed cells from the top of the head until we removed half of the worm. If there was any overgrowth on the top part of the worm before the cut, those cells were also removed. If there was no overgrowth, 1054 cells (50.19%) were removed. This cut happens at the cycle $CutTime = 60$. The simulation runs for 100 cycles, therefore there were 40 cycles left in which the model could regrow any missing cells.

We decided to vary some parameters that we hypothesized could be relevant to the performance of the task. First, we varied the number of packets created at each cycle $PacketFreq \in \{25, 28, 31\}$. Previously, we verified that increasing the number of packets produced at each cycle increases the capacity of the model for regeneration until the number of redundant packets is greater than the new ones,

Carole Knibbe et al, eds., Proceedings of the ECAL 2017, Lyon, France, 4-8 September 2017,
(Cambridge, MA: The MIT Press, ©2017 Massachusetts Institute of Technology).

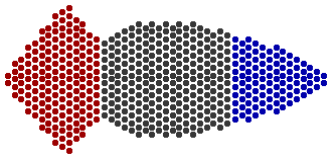

Figure 2: Shape of the topmost layer of the worm with 525 cells. Red cells belong to the head, gray cells belong to the body and blue cells are from the tail.

maintaining an asymptote. We expected the same behavior when noise was added to packets. However, we expected that it would also increase the overgrowth due to a higher probability of more packets containing noise that would create cells in locations with no previous cells.

We varied the number of bends – vectors inside a packet – before a packet backtracks $MinBends \in \{3, 5, 7\}$. We expected a positive correlation between $MinBends$ and $RegenerationRatio$. Because packets with a higher value of $MinBends$ have more vectors, there was a higher probability of noise affecting the direction or distance of those packets, possibly causing more overgrowth. Another parameter responsible for modifying patterns of navigation is the probability of a packet changing direction $BendProb$. A lower value of this parameter represents packets with longer vectors, i.e., moving across more cells in the same direction. We varied $BendProb \in \{0.1, 0.2, 0.3\}$ and we expected a negative correlation between $BendProb$ and $RegenerationRatio$. In order to regenerate cells located far from the edges of the cut, it is necessary for packets to move through a long straight path. We also expected a negative correlation between $BendProb$ and Sim due to the fact that if noise caused a packet to change direction, then a larger overgrowth could happen.

Finally, we varied both noise parameters $\sigma_{DistanceNoise}$ and $\sigma_{DirectionNoise}$. We wanted to verify the model performance for simulations either with both noise elements applied to packets or to just one of them. We also ran simulations where no noise was applied as the baseline. Thus, we varied $\sigma_{DistanceNoise} \in \{0, 0.33\}$ and $\sigma_{DirectionNoise} \in \{0, 0.25\}$. We expected that increasing noise would decrease both $RegenerationRatio$ and Sim because packets would not backtrack through the paths they came from, therefore losing shape information and moving to incorrect areas. For each point in the parameter space we ran 100 distinct simulations, resulting in a total of 10800 simulations.

Results of Experiments with Packets Containing Noise

Our results showed that while 1752 (out of 2700) simulation runs with no noise were capable of fully regenerating the worm's shape, no runs with noise could totally regenerate the structure. The maximum value found for $RegenerationRatio$ on simulations which contained noise was 91.236. Table 1 shows the average value and standard deviation for each pair of $\sigma_{DistanceNoise}$ and $\sigma_{DirectionNoise}$. As the value of $\sigma_{DistanceNoise}$ is higher than $\sigma_{DirectionNoise}$, there is more noise applied to the length of the packets' vectors than to their directions. Looking at the results for Sim in Table 2, we can see that these noise levels led to a very high overgrow. For example, the combination of both noise types led to an average similarity of 19.6%, i.e., a shapeless structure existed at the end of simulation. Some examples of simulation runs can be seen in Figure 3. Figure 3a shows a completely regenerated worm with no overgrowth ($Sim = 1$) while Figure 3b shows the most similar worm after noise ($Sim = 0.828$, $\sigma_{DistanceNoise} = 0$ $\sigma_{DirectionNoise} = 0.25$) and Figure 3c shows the least similar worm ($Sim = 0.181$, $\sigma_{DistanceNoise} = 0.33$ $\sigma_{DirectionNoise} = 0.25$).

Dis \ *Dir*	**0**	**0.25**
0	$99.004\% \pm 2.468\%$	$79.711\% \pm 4.014\%$
0.33	$66.287\% \pm 4.135\%$	$64.137\% \pm 3.727\%$

Table 1: Average $RegenerationRatio$ for all combinations of noise applied on packets.

Dis \ *Dir*	**0**	**0.25**
0	0.990 ± 0.023	0.616 ± 0.099
0.33	0.219 ± 0.016	0.196 ± 0.013

Table 2: Average Sim for all combinations of noise applied on packets.

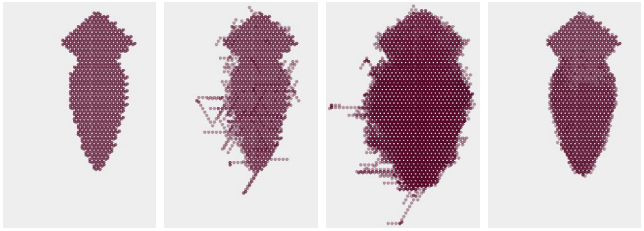

(a) (b) (c) (d)

Figure 3: A dorsal view of the simulated worm structure in four different simulation runs. (a) $Sim = 1$ (b) $Sim = 0.828$ (c) $Sim = 0.181$ (d) $Sim = 0.664$

We performed two ANOVAs with $PacketFreq$, $MinBends$, $BendProb$, $\sigma_{DistanceNoise}$, $\sigma_{DirectionNoise}$ as independent variables and $RegenerationRatio$ and Sim as dependent variables. The ANOVA for $RegenerationRatio$ showed significant main effects for all variables ($p < .001$). It also showed significant two-way interactions between all variables and

Carole Knibbe et al, eds., Proceedings of the ECAL 2017, Lyon, France, 4-8 September 2017,
(Cambridge, MA: The MIT Press, ©2017 Massachusetts Institute of Technology).

three-way interactions with all combinations other than ($PacketFreq$, $BendProb$, $\sigma_{DistanceNoise}$) and ($PacketFreq$, $MinBends$, $\sigma_{DirectionNoise}$) (all p's $< .001$). The ANOVA also showed a four-way interaction with the combination of ($MinBends$, $BendProb$, $\sigma_{DistanceNoise}$, $\sigma_{DirectionNoise}$) ($p < .001$).

Figure 4a shows the interactions between the three independent variables ($PacketFreq$, $MinBends$ and $BendProb$) on $RegenerationRatio$ for the four combinations of noise. Our first conclusion from these results is that, different from what we expected, increasing the value of $PacketFreq$ did not increase $RegenerationRatio$ when noise was applied on packets. When no noise was applied on packets, we find the positive correlation between $PacketFreq$ and $RegenerationRatio$. We can also see that for simulations with $\sigma_{DistanceNoise} \neq 0$, increasing $PacketFreq$ did not significantly change the average $RegenerationRatio$. However, if $\sigma_{DirectionNoise} = 0.25 \wedge \sigma_{DistanceNoise} = 0$, increasing the number of packets decreased $RegenerationRatio$. This can be explained by the fact that $\sigma_{DistanceNoise}$ does not change the path traversed by packets, therefore, missing cells in the path are regenerated, maintaining the same $RegenerationRatio$. On the other hand, $\sigma_{DirectionNoise}$ changes the direction of backtracking packets, consequently a long path could be lost. In summary, increasing $PacketFreq$ increased overgrowth before the cut, hence increasing the number of cells that needed to be regenerated after the cut. However, due to packets changing direction, some of these cells were not regenerated, reducing $RegenerationRatio$.

The number of bends before backtracking was very important to $RegenerationRatio$ because more bends led to packets discovering a larger area of the structure, therefore regenerating more missing cells. However, when $\sigma_{DirectionNoise} \neq 0 \wedge \sigma_{DistanceNoise} = 0$, increasing the value of $MinBends$ increased the probability of packets moving to different directions than they came from. Hence, increasing $MinBends$ decreased $RegenerationRatio$. Finally, as expected, we found a negative correlation between $BendProb$ and $RegenerationRatio$. We found that for packets with no noise, $BendProb = 0.2$ is almost sufficient to fully regenerate the worm. Moreover, increasing $BendProb$ was more detrimental to simulations that contained noise on packet distances due to the fact that $BendProb$ has a direct influence on the length of packets.

The second ANOVA for Sim showed significant main effects for all variables ($p < .001$). It showed significant two-way interactions between all variables other than ($PacketFreq$, $\sigma_{DistanceNoise}$) ($p < .001$). It also showed significant three-way interactions among all combinations of variables other than ($PacketFreq$, $MinBends$, $\sigma_{DirectionNoise}$) and ($PacketFreq$, $BendProb$, $\sigma_{DirectionNoise}$) ($p < .001$). And we obtained significant four-way interactions for ($PacketFreq$, $MinBends$, $BendProb$, $\sigma_{DistanceNoise}$), ($PacketFreq$, $MinBends$, $BendProb$, $\sigma_{DirectionNoise}$) and ($MinBends$, $BendProb$, $\sigma_{DistanceNoise}$ $\sigma_{DirectionNoise}$) ($p < .001$). Finally, it showed a significant five-way interaction among all variables ($p < .001$).

Looking at the interactions between the independent variables and Sim (Figure 4b), we first verified that the frequency of packets did not increase the average similarity of the worm when there was no noise applied to packets. However, increasing $PacketFreq$ was detrimental to the Sim because a higher value of $PacketFreq$ led to a higher number of new cells (overgrowth) due to packets moving across wrong paths. In general, increasing the number of bends before backtracking aid worm similarity because all cells that existed since the beginning of the simulation are transmitting new packets. In addition, if packets have more bends, then they describe a larger area of the structure, thereafter regenerating more missing cells. However, when packets contained noise on their directions, increasing the number of bends increased the probability that packets backtracking in wrong directions, consequently creating cells outside the original bounds of the worm and reducing Sim. Finally, in order to fully regenerate the worm, it is necessary that packets created by cells on the top of the worm reach the edge of the cut. This behavior requires packets with longer vectors. For that reason, in experiments with no noise increasing the value of $BendProb$ decreased the final similarity of the worm (i.e., fewer cells were regenerated). In experiments with noise applied to distance of the vectors, increasing the value of $BendProb$ was bad, but not as detrimental to the performance as in experiments with no noise. This is explained by the fact that although high values of $BendProb$ led to shorter packets, the noise could increase the distance of this packet, therefore regenerating a cell that would not regenerate otherwise. However, in experiments with noise applied only to the direction of the vectors, longer packets (low $BendProb$) were detrimental because when packets located close to the edges changed direction, they created new cells in locations where there were no cells in the original worm.

Experiments with the Activation Mechanism

In the previous section, we showed that applying Gaussian noise on packets, as expected, reduced the reliability of the model, thus making it impossible fully regenerate the worm. Hence, the question that arises is the following: what could be the evolved mechanisms that may lead organisms to continue their regeneration even when cell-cell communication is error-prone? We hypothesized that organisms could have an "activation" mechanism by which cells only regenerate missing cells if they receives various packets confirming the previous existence of the missing cell. To validate our hypothesis, we modified our model to account for this activation mechanism. Each location (x, y, z) that could contain

Carole Knibbe et al, eds., Proceedings of the ECAL 2017, Lyon, France, 4-8 September 2017,
(Cambridge, MA: The MIT Press, ©2017 Massachusetts Institute of Technology).

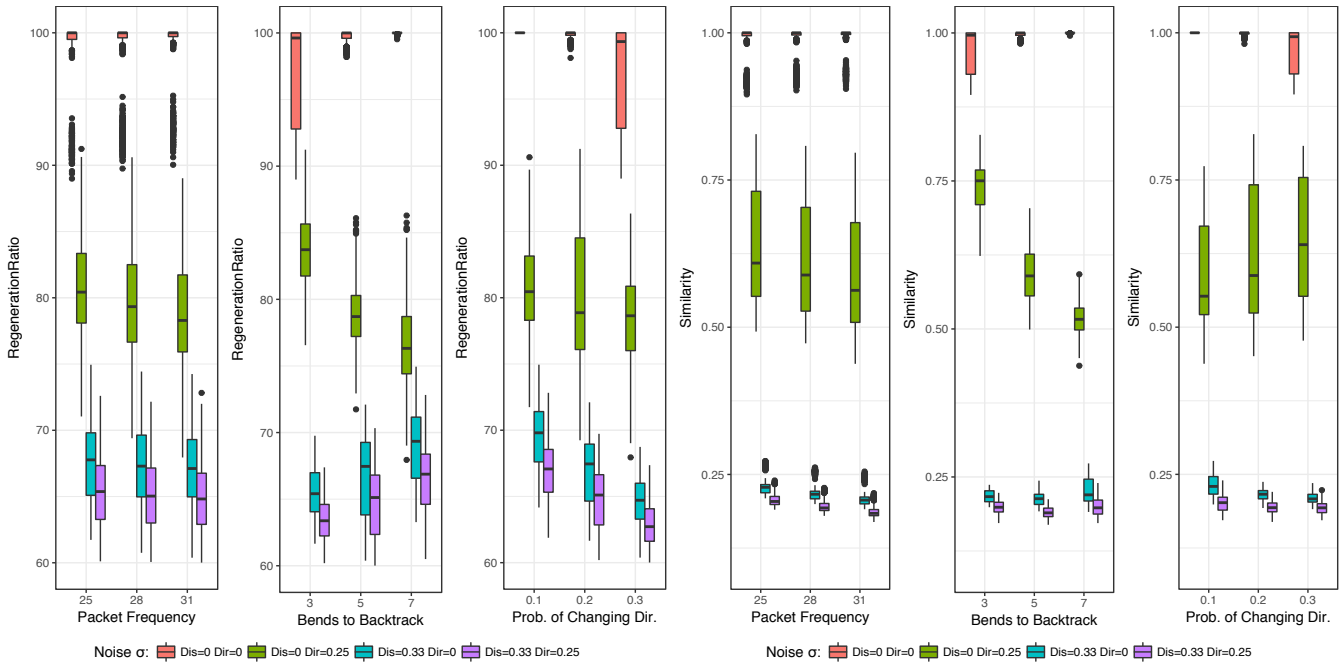

(a) Box plots of the independent variables ($PacketFreq$, $MinBends$ and $BendProb$) and $RegenerationRatio$ for all types of noise.

(b) Box plots of the independent variables ($PacketFreq$, $MinBends$ and $BendProb$) and Sim for all types of noise.

Figure 4: Distribution of the interaction between the three independent variables and the two performance metrics ($RegenerationRatio$ and Sim).

a cell has an activation value $c_{act}^{(x,y,z)}$ between 0 and 1. If $c_{act}^{(x,y,z)} \geq 1$, then there is an alive cell located in position (x, y, z), otherwise there is no cell in this position.

The backtrack mechanism now works as follows. When a cell c in location (x, y, z) backtracks a packet to a location (x', y', z'), the cell checks if there is an alive cell in (x', y', z'). If there is an alive cell to receive the packet, the packet continues its path. Otherwise, a new cell is not immediately regrown, but the activation in $c_{act}^{(x',y',z')}$ is increased by a value β_{act}. If $c_{act}^{(x',y',z')} \geq 1$, then the cell regrows another cell at (x', y', z') and the packet is subsequently forwarded. At the end of each cycle, a decay value δ_{act} is subtracted from all $c_{act}^{(x,y,z)}$. Thus, various packets need to quickly reach a location to regrow a new cell there. Equation 3 more formally details the activation update for each (x, y, z) and at each cycle i.

$$c_{act}^{(x,y,z)} = (\Sigma_0^{|c^i_{ReceivedPackets}|}\beta_{act}) - \delta_{act} \qquad (3)$$

where $c^i_{ReceivedPackets}$ is the list of received packets by location (x, y, z) at cycle i.

We wanted to explore the same parameter space we previously explored in experiments with noise, but now with a new dimension where we inserted the activation mechanism. Thus, we ran simulations with the same parameters described in the previous experiments but varied $\beta_{act} \in \{0.2, 0.34, 1\}$ and fixed $\delta_{act} = \frac{\beta_{act}}{5}$. For $\beta_{act} = 1$, the simulation worked exactly the same way as with no activation level. We used those runs as the baseline.

Since the simulated worms now need more packets to regrow new cells with low values of β_{act}, we expected a negative correlation between β_{act} and the extent of overgrowth on the shape of the worm. However, low values of β_{act} could lead to more difficulty in regenerating cells far from the location of the cut (i.e., cells on top of the head). Thus, we expected a moderate value of β_{act} to perform best regarding the $RegenerationRatio$ and Sim. For each point in the parameter space, we ran 100 simulations with different random seeds, resulting in a total of 32400 simulations.

Results of Experiments with the Activation Mechanism

There were 8100 simulations with no noise applied on packets (2700 runs for each possible value of β_{act}). From these simulations, 3189 were capable of completely regenerating the worm. Although this mechanism reduced the proportion of simulations that fully regenerated the worm with no noise applied on packets, in 1400 out of 24300 simulations with noise the worm was totally regrown. However, all of these fully regrown simulations happened with noise applied only on the direction of packets. Table 3 shows the average $RegenerationRatio$ and standard deviation for all val-

Carole Knibbe et al, eds., Proceedings of the ECAL 2017, Lyon, France, 4-8 September 2017,
(Cambridge, MA: The MIT Press, ©2017 Massachusetts Institute of Technology).

ues of noise applied on packets after adding the activation mechanism. Comparing with previous results, we can confirm that the activation mechanism was a little detrimental for simulations with no noise, but it increased performance of simulations that contained any noise. The same conclusion is valid for Sim as shown in Table 4. For example, Figure 3d shows the least similar worm after adding the activation mechanism ($Sim = 0.664$, $\sigma_{DistanceNoise} = 0.33$ $\sigma_{DirectionNoise} = 0.25$ and $\delta_{act} = 0.34$). In summary, this activation mechanism reduced the level of overgrowth.

Dis \ Dir	**0**	**0.25**
0	$92.499\% \pm 12.251\%$	$86.066\% \pm 12.347\%$
0.33	$75.867\% \pm 12.282\%$	$74.891\% \pm 12.691\%$

Table 3: Average $RegenerationRatio$ for all combinations of noise with addition of the activation mechanism.

Dis \ Dir	**0**	**0.25**
0	0.933 ± 0.104	0.809 ± 0.176
0.33	0.563 ± 0.257	0.552 ± 0.265

Table 4: Average Sim for all combinations of noise with addition of the activation mechanism.

Figure 5 shows the distribution of β_{act} and both dependent variables ($RegenerationRatio$ and Sim) for all combinations of noise applied to packets. As expected, we found that increasing the value of β_{act} increased the ratio of cells regenerated in simulations with no noise applied to packets. On the other hand, increasing the value of β_{act} decreased $RegenerationRatio$ when there was noise on the length of the packets' vectors. However, looking at simulation runs with $\beta_{act} < 1$, and noise applied only to the direction of the packets, we found the same result from runs with no noise. This is evidence that an activation mechanism could be important for the regeneration process in order to fix errors on the directions of packets. Looking at the value of Sim, when there was noise applied to packets, a lower value of β_{act} reduced the overgrowth and improved the similarity of the final worm to the original one. On the other hand, when there was no noise, it was harder to regrow cells located far from the cut, therefore it reduced the similarity of the final worm.

Discussion

In planarians, only adult stem cells (called neoblasts) can create and differentiate into any cell type Lobo et al. (2012). Instead, in our model any cell can create a new cell. Thus, the results show that when there is noise applied to packets, each new cell in a wrong location increases the likelihood of an even larger overgrowth. For instance, the worm sends $2100 \times PacketFreq$ packets per cycle. If one new cell grows in a wrong location, then at each cycle after that

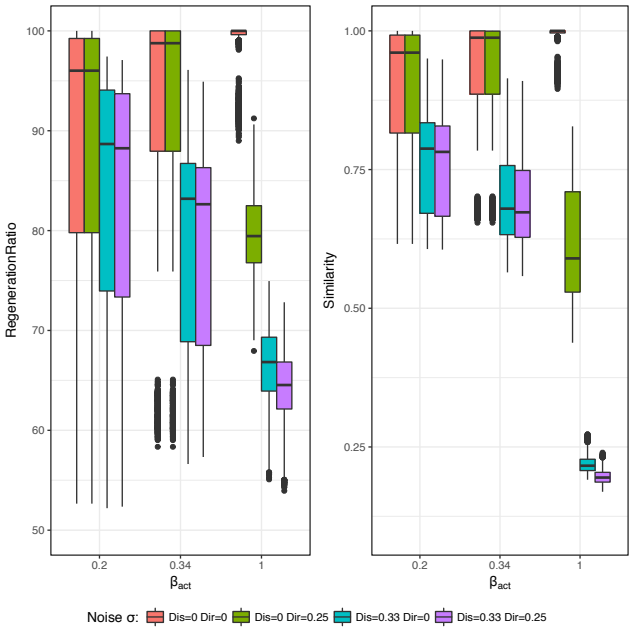

Figure 5: Distribution of the interaction between β_{act} and the two performance metrics ($RegenerationRatio$ and Sim).

the worm sends $2101 \times PacketFreq$ packets, which has a higher chance of inaccurate creating another cell.

The reliability of our model is based on shape information existing across the network of cells. Moreover, this information has a high degree of partial redundancy (i.e., various packets could regrow the same cell, even though they do not traversed the same path). Partial redundancy is very common and important in natural organisms because it preserves the organism against a variety of damages in its body or even genes (Brodsky, 2015). The inherent partial redundancy of our model allow various packets to reach locations of missing cells, thus improving the performance of our model when there is noise applied to packets. Therefore, a method for confirming evidence from different sources within a given time span before regenerating cells like the activation mechanism we proposed might have evolved in organisms with regeneration capabilities. This is a concrete model prediction that might be able to guide future biological research.

Conclusion

As a first step towards finding a mapping between our cell-cell communication mechanism of cell regeneration and a possible biological equivalent, we modified our previous model to account for noise that could occur on cellular communication. In an initial set of experiments we verified that noise was very detrimental to the overall performance of the model, not only with respect to the ratio of regenerated cells

Carole Knibbe et al, eds., Proceedings of the ECAL 2017, Lyon, France, 4-8 September 2017,
(Cambridge, MA: The MIT Press, ©2017 Massachusetts Institute of Technology).

but also the similarity of the final worm compared to the original worm. We then presented an activation mechanism which improved the performance of the model in configurations where noise existed – the first steps toward modeling the robustness observed in regenerative biological systems.

In the future, we intend to confirm whether our model can replicate other aspects that *in vivo* worms show. For example, gap junctional communication (GJC) can be inhibited through contact with alcohols such as octanol. This isolation in GJC leads to the creation of another head in the posterior part of the worm (Nogi and Levin, 2005). A first step towards replicating this result could be to generate "mirror image" packets that would create a head instead of a tail. Another direction would be to investigate the limits of regeneration based on the shape of the organism. For instance, we hypothesize that more bends would be necessary to regrow a complex limb compared to the planarian body which has fewer corners and turns in the shape. Finally, it would be interesting to extend the model to other biological processes such as the growth of tumors and anatomical remodeling.

References

Birnbaum, K. D. and Alvarado, A. S. (2008). Slicing across kingdoms: regeneration in plants and animals. *Cell*, 132(4):697–710.

Brodsky, M. (2015). Partial redundancy and morphological homeostasis: Reliable development through overlapping mechanisms. In *Proceedings of the 13th Europen Conference on Artificial Life (ECAL)*, pages 59–66. MIT Press.

Bubenik, G. A. (1990). The role of the nervous system in the growth of antlers. In *Horns, pronghorns, and antlers*, pages 339–358. Springer.

Chernet, B. and Levin, M. (2013). Endogenous voltage potentials and the microenvironment: bioelectric signals that reveal, induce and normalize cancer. *Journal of clinical & experimental oncology*.

Durant, F., Morokuma, J., Fields, C., Williams, K., Adams, D. S., and Levin, M. (2017). Long-term, stochastic editing of regenerative anatomy via targeting endogenous bioelectric gradients. *Biophysical Journal*, 112(10):2231 – 2243.

Ferreira, G. B. S., Smiley, M., Scheutz, M., and Levin, M. (2016). Dynamic structure discovery and repair for 3d cell assemblages. In *Proceedings of the Fifteenth International Conference on the Synthesis and Simulation of Living Systems (ALIFEXV)*.

Herrera-Rincon, C., Guay, J. A., and Levin, M. (2017). Bioelectrical coordination of cell activity toward anatomical target states: an engineering perspective on regeneration. In Gardiner, D. M., editor, *Regenerative Engineering and Developmental Biology: Principles and Applications*. Taylor and Francis.

Higgins, G. M. (1931). Experimental pathology of the liver. *Arch. Pathol.*, 12:186–202.

Huang, S., Ernberg, I., and Kauffman, S. (2009). Cancer attractors: A systems view of tumors from a gene network dynamics and developmental perspective. *Seminars in Cell & Developmental Biology*, 20(7):869 – 876.

Levin, M. (2012). Morphogenetic fields in embryogenesis, regeneration, and cancer: non-local control of complex patterning. *Biosystems*, 109(3):243–261.

Levin, M. (2013). Reprogramming cells and tissue patterning via bioelectrical pathways: molecular mechanisms and biomedical opportunities. *Wiley Interdisciplinary Reviews: Systems Biology and Medicine*, 5(6):657–676.

Levin, M. (2014). Endogenous bioelectrical networks store non-genetic patterning information during development and regeneration. *The Journal of physiology*, 592(11):2295–2305.

Lobo, D., Beane, W. S., and Levin, M. (2012). Modeling planarian regeneration: a primer for reverse-engineering the worm. *PLoS Comput Biol*, 8(4):e1002481.

Lobo, D., Solano, M., Bubenik, G. A., and Levin, M. (2014). A linear-encoding model explains the variability of the target morphology in regeneration. *Journal of The Royal Society Interface*, 11(92):20130918.

Morgan, T. H. (1898). Experimental studies of the regeneration of planaria maculata. *Development Genes and Evolution*, 7(2):364–397.

Nogi, T. and Levin, M. (2005). Characterization of innexin gene expression and functional roles of gap-junctional communication in planarian regeneration. *Developmental biology*, 287(2):314–335.

Oviedo, N. J., Morokuma, J., Walentek, P., Kema, I. P., Gu, M. B., Ahn, J.-M., Hwang, J. S., Gojobori, T., and Levin, M. (2010). Long-range neural and gap junction protein-mediated cues control polarity during planarian regeneration. *Developmental biology*, 339(1):188–199.

Owlarn, S. and Bartscherer, K. (2016). Go ahead, grow a head! a planarian's guide to anterior regeneration. *Regeneration*.

Price, J. S., Allen, S., Faucheux, C., Althnaian, T., and Mount, J. G. (2005). Deer antlers: a zoological curiosity or the key to understanding organ regeneration in mammals? *Journal of Anatomy*, 207(5):603–618.

Soto, A. M. and Sonnenschein, C. (2005). Emergentism as a default: cancer as a problem of tissue organization. *Journal of biosciences*, 30(1):103–118.

Sullivan, K. G., Emmons-Bell, M., and Levin, M. (2016). Physiological inputs regulate species-specific anatomy during embryogenesis and regeneration. *Communicative & integrative biology*, 9(4):e1192733.

Umesono, Y., Tasaki, J., Nishimura, Y., Hrouda, M., Kawaguchi, E., Yazawa, S., Nishimura, O., Hosoda, K., Inoue, T., and Agata, K. (2013). The molecular logic for planarian regeneration along the anterior-posterior axis. *Nature*, 500(7460):73–76.

Werner, S., Stückemann, T., Amigo, M. B., Rink, J. C., Jülicher, F., and Friedrich, B. M. (2015). Scaling and regeneration of self-organized patterns. *Physical review letters*, 114(13):138101.

Carole Knibbe et al, eds., Proceedings of the ECAL 2017, Lyon, France, 4-8 September 2017,
(Cambridge, MA: The MIT Press, ©2017 Massachusetts Institute of Technology).